



Integrating biochar and water-saving irrigation: A key strategy for effective phosphorus management in rice cultivation



Suting Qi^a, Shufang Wang^b, Shihong Yang^{a,*1}, Pengfei Zhang^a, Qian Huang^a, JingCheng Zhu^a, Jin Li^a, Zewei Jiang^a, Yi Xu^a, Jie Zhang^a, Lili Zhu^c

^a College of Agricultural Science and Engineering, Hohai University, Nanjing, PR China

^b College of Water Conservancy, Yunnan Agricultural University, Kunming, PR China

^c Kunshan Water Affairs and Hydrological Dispatching Center, Suzhou, PR China

ARTICLE INFO

Keywords:

P fractionation

Water-saving irrigation

Biochar

P leaching loss

ABSTRACT

As a promising technology for water-saving, pollution reduction, and increased yield in rice paddies, application of water-saving irrigation and biochar in rice fields may potentially address the issues of low phosphorus utilization efficiency and increased phosphorus surplus, which heightens phosphorus loss. However, the efficacy of this approach remains uncertain. This study, grounded in a two-year field experiment, investigated the distribution of various phosphorus forms in both solid and liquid phases under biochar application in water-saving irrigated rice paddies, and examined phosphorus uptake by rice plants, as well as phosphorus leaching loss characteristics. The solid-phase analysis revealed partially labile phosphorus (51.82–73.03 % of total phosphorus), particularly dil.HCl-P (67.86–89.57 %), as the dominant soil phosphorus pool. Biochar application showed distinct temporal effects. In the first year, 20 and 40 t ha⁻¹ applications increased total phosphorus content across soil profiles by 4.91–17.40 %. However, second-year observations showed significant decreases (1.07–21.79 %) due to activation of partially labile phosphorus and stable phosphorus in soil. Soil solution monitoring identified molybdate-reactive phosphorus (37.88–95.76 % of total phosphorus) as the most dynamic fraction, while 40 t ha⁻¹ biochar consistently elevated solution total phosphorus concentrations (2.52–4.36 % increase). The 20 t ha⁻¹ biochar combined with water-saving irrigation emerged as the optimal strategy, effectively balancing phosphorus availability for plant uptake while minimizing environmental losses (0.04–1.13 % decrease of total phosphorus in soil solution) in southern China. Future research should incorporate more biochar application rates and extended observation periods to fully validate the sustainability of this coupled approach. Our findings, based on a two-year experiment, show promising short-term benefits for water and phosphorus use efficiency, suggesting a pathway towards more sustainable management practices.

1. Introduction

The future of agriculture necessitates more efficient and effective phosphorus (P) use, characterized by a higher P use efficiency (Kruse et al., 2015). In paddy fields where the annual utilization rate of P fertilizers is merely 10–20 % (Wu et al., 2018), it is imperative to adopt appropriate soil P management strategies to prevent P deficiency in rice and to minimize the excessive P runoff into aquatic ecosystems (Liu et al., 2013). Biochar, often referred to as “soil armor,” has been widely demonstrated as an effective technology for enhancing paddy field productivity, optimizing fertilizer use, and reducing emissions (Jia et al.,

2024; Wang et al., 2024). Its superiority in increasing the efficacy of P availability and reducing P losses in paddy fields has been noted. For instance, Abdala et al. (2015) indicated that the application of biochar increased the abundance of P-solubilizing microorganisms in flooded rice paddies, thereby enhancing P availability. Furthermore, Miao et al. (2023) found that biochar effectively retained P nutrients in flooded rice fields under various rainfall intensities, thereby mitigating P loss. However, this immobilization effect may also reduce the availability of P in paddy soils. Most existing studies on biochar’s influence on P cycling in paddy fields have been limited to flooding conditions, with related research indicating that water-saving irrigation can enhance P

* Corresponding author.

E-mail address: ysh7731@hhu.edu.cn (S. Yang).

¹ State key laboratory of hydrology-water resources and hydraulic engineering, Hohai University, 8 Fochengxi Road, Jiangning District, Nanjing, 211100, China.

bioavailability. Whether the integration of biochar and water-saving irrigation can simultaneously reduce P loss while maintaining high P availability remains unexplored and requires further experimental validation.

Additionally, the composition of solid-phase P in soil determines its bioavailability and mobility (Negassa and Leinweber, 2009). To some extent, this composition directly impacts the vertical migration and fate of P in rice fields, including parameters such as P uptake by rice plants and P leaching losses. Regarding the vertical migration of P, Matin et al. (2020) showed that the concentrations of various P forms exhibit significant vertical variation with soil depth, which can be ascribed to the collective influence of physical, chemical, and biological processes. Furthermore, solid-phase P functions as a reservoir that replenishes liquid-phase P, thereby influencing the soil's P supply capacity as well as its associated environmental risks (phosphorus fate). Consequently, exploring sustainable P management strategies for rice paddies necessitates a critical need for scientific characterization and accurate understanding of soil P forms.

Hedley and Tiessen P fractionation schemes (Hedley et al., 1982a; Tiessen and Moir, 1993), the current standard for comprehensively characterizing both organic and inorganic pools, are particularly relevant for our study of paddy soils (Sun et al., 2020). However, despite their value in assessing bioavailability, these methods are labor-intensive, and existing studies applying them to paddies have primarily provided static analyses at harvest. This neglects critical spatiotemporal variations in phosphorus dynamics during rice growth stages, especially under management practices like combined water-saving irrigation and biochar application – a key knowledge gap our research addresses.

To address these gaps, a two-year observational study was carried out in biochar and water-saving irrigation treated paddy fields. This involved multi-frequency, multi-depth, and multi-season field sampling of the experimental plots. Sequential fractionation was employed to characterize the P fractionation in the solid phase of the paddy soil, thereby elucidating the patterns of P distribution across various soil depths under combined water-saving irrigation and biochar amendment. Concurrently, we monitored P leaching losses and the P uptake by rice plants to quantify the P dynamics within the paddy ecosystem. The objective of this study is to tackle the following research inquiries: (i) Determine how biochar and water-saving irrigation influence the distribution of solid-phase P fractions in paddy soils. (ii) Assess the impact of these treatments on P leaching losses and rice P uptake. (iii) Evaluate the temporal dynamics and stability of P changes across two years. This study investigates critical challenges in sustainable agriculture by integrating agronomic and environmental perspectives, with a focus on P dynamics. From an agronomic standpoint, we examine P uptake efficiency in crops, while environmentally, we address the pressing issue of P leaching. The excessive leaching of P represents a dual challenge: it significantly diminishes crop nutrient utilization efficiency while concurrently contributing to aquatic ecosystem degradation through eutrophication - a growing global environmental concern. Enhancing P use efficiency aligns with international initiatives promoting sustainable agricultural resource management, serving as a crucial strategy to simultaneously address food security demands and ecological conservation imperatives. By elucidating the intricate balance between agricultural productivity and environmental protection, this research provides valuable scientific insights for developing sustainable agricultural practices.

2. Materials and methods

2.1. Experimental site and design

The experiment was conducted at the Kunshan Drainage and Irrigation Experiment Station ($34^{\circ}15'21''$ N, $121^{\circ}05'22''$ E) from June 29, 2022 (rice transplanting) to October 24, 2022 (rice harvesting), and

from June 28, 2023 (rice transplanting) to October 22, 2023 (rice harvesting). Temperature and rainfall of the experimental site during the two-year trial were shown in Fig. S1. The experimental site was equipped with 12 drainage lysimeters (2.0 m width \times 2.5 m length), each fitted with rain shelters to exclude rainfall and regulate drainage volume. This study employed two irrigation methods: controlled irrigation (C) and flooding irrigation (F). Within the water-saving irrigation treatment, three levels of biochar were applied: 0 t ha^{-1} (A), 20 t ha^{-1} (B), and 40 t ha^{-1} (C). The flooding irrigation treatment served as a control without biochar application, resulting in a total of four treatments designated as CA, CB, CC, and FA (Table S1). Each treatment has three replications. All treatments are arranged in a randomized order. The rate of 20 t ha^{-1} and 40 t ha^{-1} represents moderate and high application scenarios that bracket the range commonly used in rice cultivation while remaining economically viable for farmers (Jiang et al., 2021b). According to prior research by our team, daily percolation rates under water-saving irrigation and flooding irrigation were approximately 3 mm d^{-1} and 5 mm d^{-1} , respectively. Manual drainage was conducted daily at 18:00 via subterranean access corridors.

Prior to rice transplanting in 2022, the biochar used in the experiment was applied as a single soil amendment at a depth of 0–20 cm. The initial properties of the biochar used in the experiment and the soil in the lysimeters have been detailed in our previous studies (Qi et al., 2024). The type of biochar employed was derived from wheat straw, produced under anaerobic conditions at a heating rate of $7.5^{\circ}\text{C min}^{-1}$ and a temperature of 600°C . The fundamental properties of the biochar are as follows: it has a particle size of 200 μm , an organic matter content of 78 %, a specific surface area of $683 \text{ m}^2 \text{ g}^{-1}$, an available P content of 1.3 g kg^{-1} , and an available potassium content of 23.3 %. The rice variety employed in this case was Nanjing 46 Japonica. The spacing between rows and plants during planting is 13.0 cm and 25.0 cm, respectively. Fertilization in the lysimeters was conducted in accordance with the local fertilization standards in Kunshan. Specific fertilization rates are detailed in the table (Table S1).

2.2. Soil sampling and analysis

A comprehensive multi-season, multi-depth sampling strategy was implemented to capture spatiotemporal dynamics: Soil samples were collected across four critical growth stages in 2023 (June 23, July 31, September 1, October 20) and three key phases in 2022 (July 31, August 28, October 20), using the five-point mixing method. Stratified sampling was conducted with in-situ soil samplers at 20-cm depth intervals from 0–60 cm (0–20, 20–40, 40–60 cm), enabling high-resolution vertical profiling. All samples underwent rigorous P fractionation via Tiessen's sequential extraction protocol. After removing impurities such as roots or stones, all collected soil samples were air-dried, sieved, and then subjected to measurements.

The specific steps for the Tiessen P sequential fractionation method are as follows (Fig. 1)(Tiessen and Moir, 1993): Initially, 0.5000 g of air-dried soil is placed in a 50 mL centrifuge tube. The soil is then sequentially extracted at room temperature using an anion exchange resin, followed by 0.5 M NaHCO₃ (NaHCO₃-P), 0.1 M NaOH (NaOH-P), and 1M HCl (dil.HCl-P), with each extraction lasting 16 h. Subsequently, the residual material is extracted with concentrated HCl (conc. HCl) by placing it in a water bath at 80°C for 10 min, followed by resting for 1 h; centrifugation then yields the conc. HCl-P fraction. Finally, the remaining residue undergoes repeated digestion with H₂SO₄-H₂O₂ at 360°C to obtain the residual-P fraction.

For the extracts from 0.5 M NaHCO₃, 0.1 M NaOH, and conc. HCl, part of the supernatant is adjusted to the appropriate pH and directly analyzed for inorganic P (P_i). Another portion of the supernatant undergoes potassium persulfate digestion under high temperature and pressure conditions before pH adjustment, after which P content is also determined using the Molybdenum blue method (Murphy and Riley, 1962). At this stage, the measured P corresponds to total P (P_t) in the

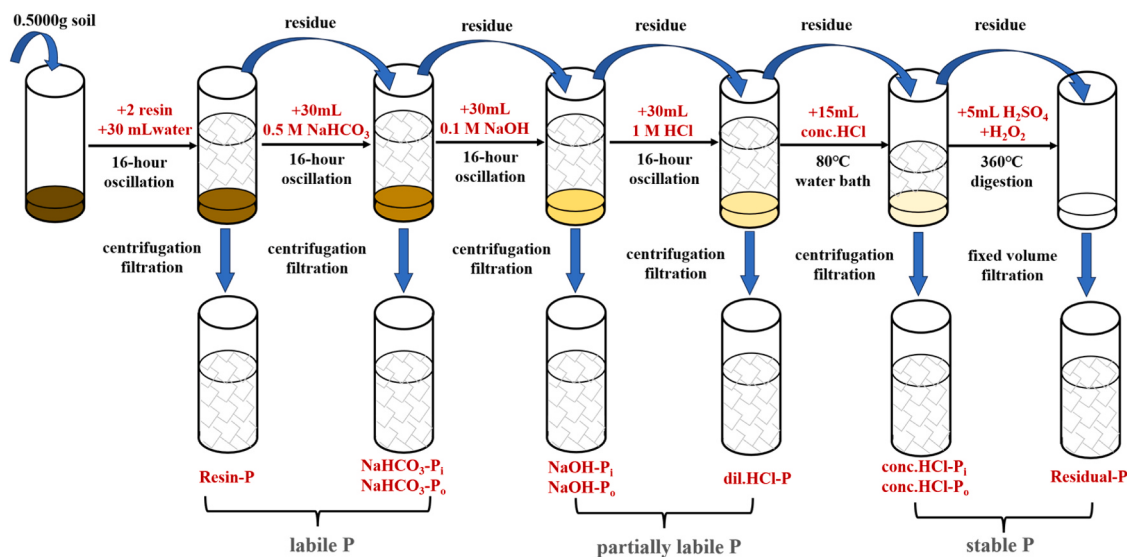


Fig. 1. Flow chart for Tiessen phosphorus sequential fractionation.

solution, while the organic P (P_o) content within the respective extracts is calculated as the difference between P_t and P_i . Total inorganic P (P_{tot}) is defined as the sum of resin-P, $NaHCO_3$ -P_i, $NaOH$ -P_i, dil.HCl-P_i, conc.HCl-P_i, and residual-P. Meanwhile, total organic P (P_{tot}) is the cumulative amount of $NaHCO_3$ -P_o, $NaOH$ -P_o, and conc.HCl-P_o.

According to the studies by Motavalli and Miles (2002) and Yang and Post (2011), different P fractionations can be broadly classified based on their bioavailability to plants. Labile P is defined as the sum of resin-P and $NaHCO_3$ -P ($P_i + P_o$); this fraction is considered directly accessible for plant uptake. In contrast, partially labile P consists of the sum of $NaOH$ -P ($P_i + P_o$) and dil.HCl-P_i. This particular fraction of P is associated with secondary iron and aluminum minerals, as well as primary calcium minerals. Although its availability is relatively low, it can still be utilized by plants after undergoing weathering and subsequent release (Yang and Post, 2011; Hou et al., 2016). Furthermore, conc.HCl-P ($P_i + P_o$) and residual-P, contribute to what is categorized as stable P. This type of P exhibits the lowest bioavailability due to its particularly low solubility (Hedley et al., 1982b; Tiessen and Moir, 1993; Condron and Newman, 2011).

2.3. Soil solution sampling and analysis

Prior to rice transplantation, three in situ soil solution samplers were installed in each lysimeter at depths of 20 cm, 40 cm, and 60 cm. A detailed description of the soil samplers has been reported in our previous research. The frequency of solution collection was as follows: after the application of basal fertilizer, samples were collected every 2 days for a total of 5–6 sampling events. Subsequently, the sampling frequency was adjusted to every 5–7 days. The collected soil solution samples were promptly sent to the laboratory for analysis. A portion of the collected solutions was directly analyzed for molybdate reactive P (MRP, inorganic P) using the molybdenum blue method. The remaining solution was subjected to potassium persulfate digestion prior to quantification of total P (TP) using the same molybdenum blue method. The amount of molybdate-unreactive phosphorus (MUP, considered as organic P) was determined by subtracting inorganic P from total P.

The P leaching loss was calculated using the following formula (kg P ha⁻¹):

$$L = \sum_{i=1}^n 0.01 \cdot C_i \cdot S_i \quad (1)$$

where L represents the cumulative phosphorus leaching loss (kg ha⁻¹), n denotes the number of samples collected, C_i indicates the phosphorus

concentration in the leachate, specifically reflecting the concentration in the soil solution at depths of 40–60 cm (mg L⁻¹), and S_i refers to the leaching intensity at the i_{th} sampling event. In this study, we established a controlled irrigation rate of 3 mm d⁻¹ for controlled irrigation and 5 mm d⁻¹ for flooding irrigation.

2.4. Rice plant sampling and analysis

During rice harvest, the portion of the rice plant above ground was gathered from each lysimeter for assessment of its P content. This aboveground biomass was divided into stems, leaves, and panicles. After being finely ground and sieved, the samples underwent digestion with a $HClO_4$ - H_2SO_4 solution. Subsequently, the P content of each component was measured using the molybdenum blue method. The total P uptake by the rice plant was computed by summing the P contents across all plant parts.

2.5. Statistical analysis

The Shapiro-Wilk test was employed to examine the normality of the data. If the data did not meet the assumptions of normality or homogeneity of variance, data transformation was performed. Differences among treatments in soil P fractions, total leaching losses of each P fraction, and average concentrations of P fractions in soil solution were analyzed using one-way ANOVA followed by Fisher's Least Significant Difference (LSD) test for multiple comparisons. Statistical significance was set at $p < 0.05$. Error bars in figures represent the standard error (SE) of the mean for three replicates per treatment. SPSS version 19.0 and Excel 2016 were used for data analysis, whereas Origin 2024 was utilized for creating graphical representations of the data.

3. Results

3.1. Spatio-temporal evolution characteristics of soil phosphorus pools

Observations of P fractionations in rice paddy soils under various treatment conditions over a two-year growth period indicate that the partially labile P fraction is the predominant component, regardless of treatment, depth, or season (Figs. 2,3). This fractionation accounts for approximately 51.82–73.03 % of the TP. Following this, the stable P comprises about 19.05–45.83 % of the TP. In contrast, the labile P, which can be directly utilized by plants, constitutes only 1.38–10.50 % of the TP. The dil.HCl-P contributes between 67.86–89.57 % to the

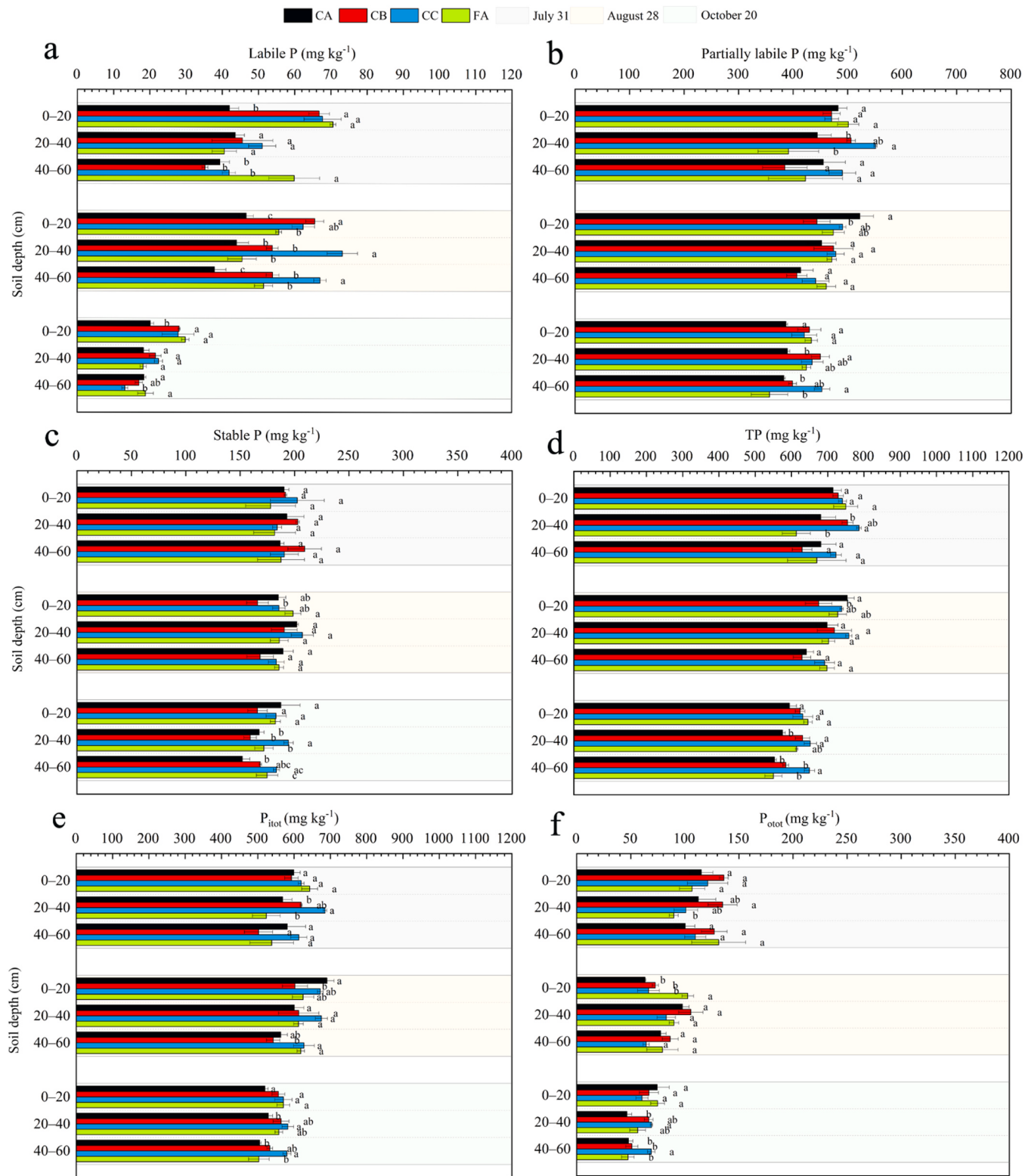


Fig. 2. Concentration of labile P (a), partially labile P (b), stable P (c), total P (d), total inorganic P (e) and total organic P (f) at different soil depth in 2022. Treatment differences are denoted by lowercase letters ($p < 0.05$), while the error bars depict the standard error based on three replicates ($n = 3$). CA: controlled irrigation +0 t ha^{-1} biochar, CB: controlled irrigation +20 t ha^{-1} biochar, CC: controlled irrigation +40 t ha^{-1} biochar, FA: flooding irrigation +0 t ha^{-1} biochar.

partially labile P, establishing it as the primary component of this fraction and the main inorganic P component. In terms of chemical composition, inorganic P, which includes Resin-P, $\text{NaHCO}_3\text{-Pi}$, $\text{NaOH}\text{-Pi}$, dil.HCl-P , conc. HCl-Pi , and Residual-P, is 2.81–32.79 times more abundant than organic P, which consists of $\text{NaHCO}_3\text{-Po}$, $\text{NaOH}\text{-Po}$, and

conc. HCl-Po . Notably, $\text{NaOH}\text{-Po}$ dominates the composition of organic P (Fig. S2, S3).

Biochar affects the temporal and spatial distribution of soil P in water-saving irrigated rice fields. In 2022, the application of biochar at rates of 20 t ha^{-1} and 40 t ha^{-1} increased TP content in soil at various

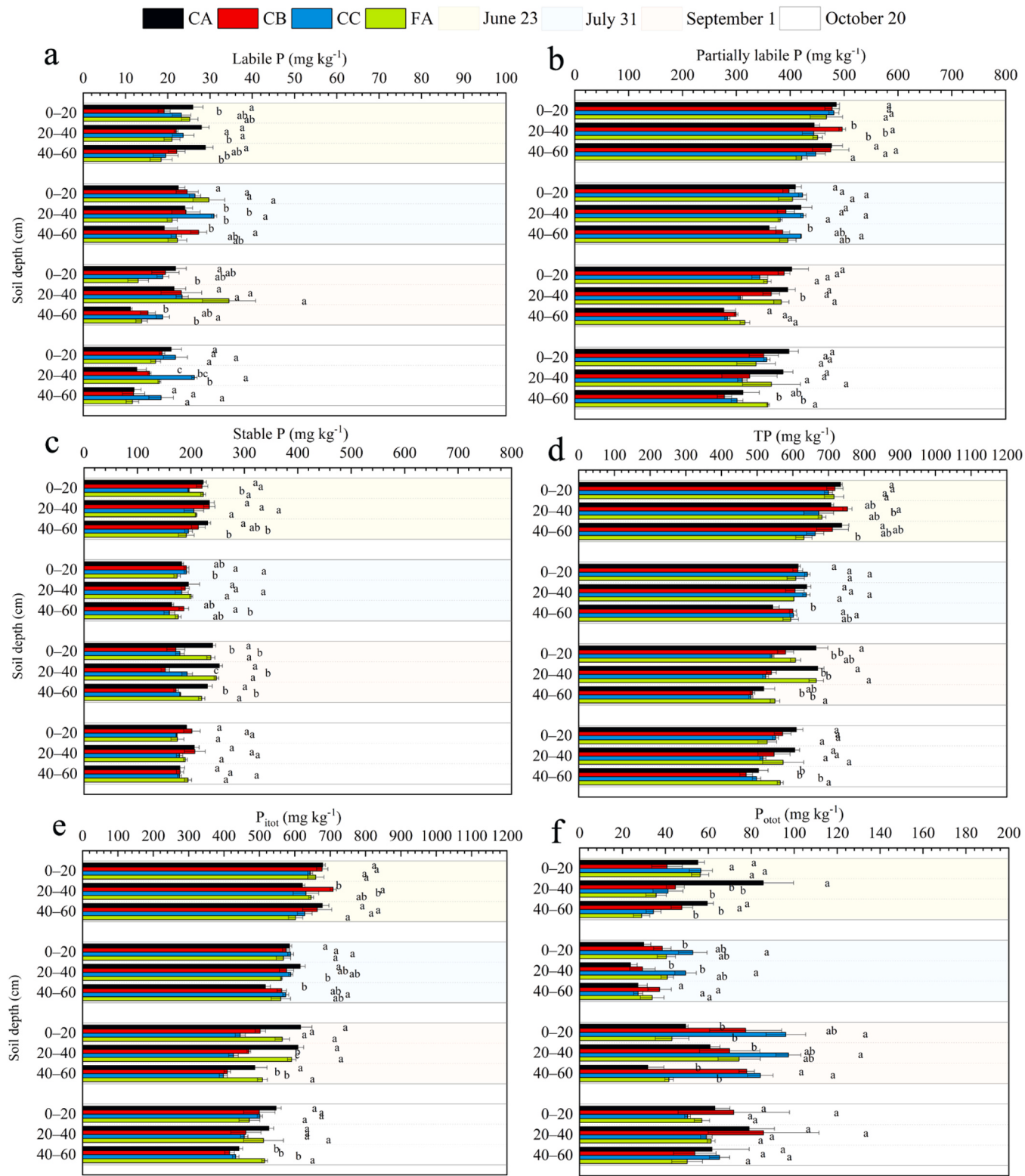


Fig. 3. Concentration of labile P (a), partially labile P (b), stable P (c), total P (d), total inorganic P (e) and total organic P (f) at different soil depth in 2023. Treatment differences are denoted by lowercase letters ($p < 0.05$), while the error bars depict the standard error based on three replicates ($n = 3$). CA: controlled irrigation +0 t ha^{-1} biochar, CB: controlled irrigation +20 t ha^{-1} biochar, CC: controlled irrigation +40 t ha^{-1} biochar, FA: flooding irrigation +0 t ha^{-1} biochar.

depths in water-saving irrigated rice fields. Compared with CA, the CB treatment on the rice harvest date (October 20) showed increases in TP content of 4.91 %, 9.61 % ($p < 0.05$), and 5.62 % at soil depths of 0–20 cm, 20–40 cm, and 40–60 cm, respectively. The CC treatment exhibited higher TP content than CA throughout the entire rice growth

period at 0–60 cm depths. Specifically, at harvest, TP content in the 0–20 cm, 20–40 cm, and 40–60 cm layers increased by 6.16 %, 13.29 % ($p < 0.05$), and 17.40 % ($p < 0.05$), respectively. For CC treatment, alongside the increase in TP content, there were concurrent increases in both labile P and partially labile P. Over the entire growth period, labile

P content in the 0–60 cm soil profile increased by 6.52–66.47 %, and partially labile P in the 20–60 cm layers increased by 5.68–24.08 %. In 2023, TP content under biochar treatments was generally lower than that of CA, especially during the mid-to-late stages of rice growth. During these stages, TP in the 0–60 cm soil layer under CB and CC treatments decreased by 6.12–19.36 % and 1.07–21.79 %, respectively, compared to CA, mainly due to reductions in partially labile P and stable P fractions. On September 1, stable P in the 0–60 cm soil layer under CB and CC treatments was reduced by 25.39–38.89 % and 22.05–25.42 %, respectively, relative to CA; by October 20, partially labile P in the 0–60 cm layer under CB and CC treatments decreased by 11.01–16.06 % and 3.47–19.51 %, respectively.

Water-saving irrigation effectively reduces P leaching to deeper soil layers by altering the distribution of P fractions. Although there was no significant difference in TP content between CA and FA treatments, water-saving irrigation significantly decreased labile P content in both surface (0–20 cm) and deep (40–60 cm) soil layers in 2022. Compared to FA, the CA treatment reduced labile P content by 16.16–40.53 % ($p < 0.05$) in the 0–20 cm layer and by 2.24–34.32 % ($p < 0.05$) in the 40–60 cm layer. The reduction in labile P was accompanied by increases in partially labile P and stable P fractions. In 2023, water-saving irrigation increased TP content in the 0–40 cm soil layer but decreased TP content in the 40–60 cm layer. At harvest (October 20), TP content in the 40–60 cm soil layer of CA-treated rice fields was significantly lower than that in FA treatment by 10.83 % ($p < 0.05$). The increase in TP within the 0–40 cm soil layer was mainly attributed to the partially labile P fraction.

3.2. Dynamics of phosphorus components in soil solution

Based on Figs. 4, 5, and 6, it is evident that biochar and irrigation regimes did not significantly influence the temporal variation patterns of TP, MUP and MRP concentrations in the soil solution. Notably, the TP concentration in the paddy soil solution exhibited minimal change over the two years of rice growth, regardless of the applied treatments. Apart from a temporary peak in TP following the application of panicle fertilizer

in 2022, no significant variations were observed during the remaining stages of that year or during the entire duration of rice growth in 2023. In 2022, the TP concentrations for the various treatments at depths of 0–20 cm, 20–40 cm, and 40–60 cm were $0.3703\text{--}0.6487 \text{ mg L}^{-1}$, $0.3771\text{--}1.0325 \text{ mg L}^{-1}$, and $0.3759\text{--}0.8050 \text{ mg L}^{-1}$, respectively. In 2023, the overall TP content in the soil solution was higher than in 2022, with concentrations at the same depths being $0.4033\text{--}0.5514 \text{ mg L}^{-1}$, $0.3757\text{--}0.5421 \text{ mg L}^{-1}$, and $0.3903\text{--}0.5492 \text{ mg L}^{-1}$, respectively. Consistent with the temporal variation pattern of TP, the concentration of MUP in the soil solution showed a noticeable peak only after the application of panicle fertilizer in 2022, with little change in concentration over time at the three depths. In contrast, MRP, which accounted for approximately 37.88–95.76 % of the soil solution TP, exhibited significant fluctuations in relation to rice growth, particularly in 2022. During that year, MRP displayed two peaks and one trough at various depths throughout the rice growth period, with peaks occurring on July 2 (immediately following P fertilizer application) and July 25, and a trough on August 23. In 2023, only one peak in MRP was observed, occurring on September 7.

Results showed that in 2022 (Table 1), the application of 20 t ha^{-1} biochar (CB treatment) significantly decreased TP in the soil solution of the surface layer (0–20 cm) by 14.89 % ($p < 0.05$), with MUP decreasing from 0.1794 mg L^{-1} to 0.1527 mg L^{-1} . Meanwhile, biochar promoted an increase of 3.80 % ($p < 0.05$) in MRP in 20–40 cm layer, indicating that biochar may facilitate downward P migration or enhance crop uptake. Data from 2023 demonstrated that CC treatment had a more pronounced effect on enhancing P contents across all soil layers: TP increased by 4.36 %, 2.52 %, and 3.08 % in the 0–20 cm, 20–40 cm, and 40–60 cm layers, respectively (all $p < 0.05$). Concurrently, MRP and MUP contents were significantly elevated by 1.46–3.01 % and 4.58–6.89 %, respectively (Table 1).

The impact of irrigation patterns on P components in the soil solution exhibited interannual variability. In the first year of observation, we identified a significant P retention effect associated with the CA treatment. This effect led to notably higher concentrations of TP and MUP in the soil solution at the 0–20 cm depth under the CA treatment compared

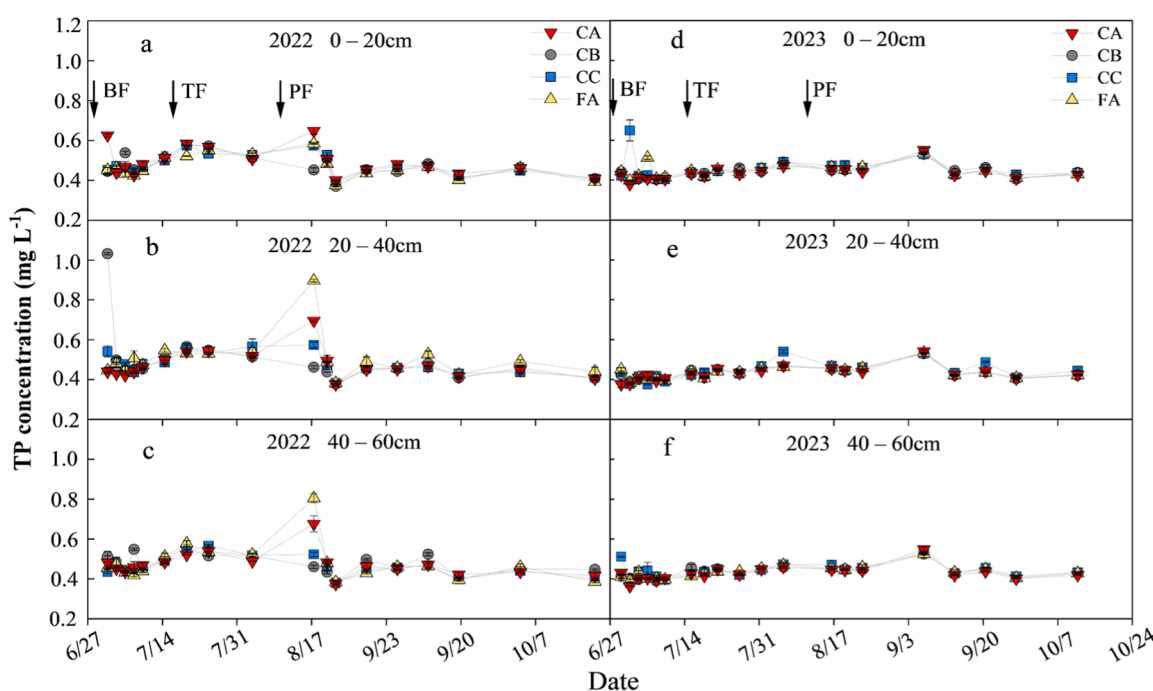


Fig. 4. Concentration of total P (TP) in soil solution at different depths in 2022 and 2023. a, d: 0–20 cm; b, e: 20–40 cm; c, f: 40–60 cm. The standard error ($n = 3$) is indicated by the error bars. CA: controlled irrigation + 0 t ha^{-1} biochar, CB: controlled irrigation + 20 t ha^{-1} biochar, CC: controlled irrigation + 40 t ha^{-1} biochar, FA: flooding irrigation + 0 t ha^{-1} biochar.

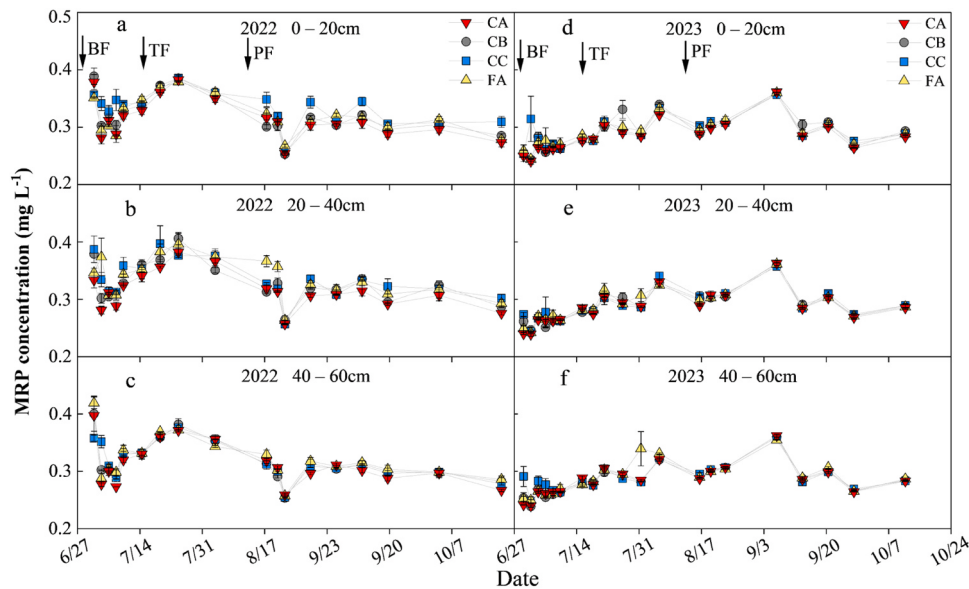


Fig. 5. Concentration of molybdate reactive P (MRP) in soil solution at different depths in 2022 and 2023. a, d: 0–20 cm; b, e: 20–40 cm; c, f: 40–60 cm. The standard error ($n = 3$) is indicated by the error bars. CA: controlled irrigation +0 t ha^{-1} biochar, CB: controlled irrigation +20 t ha^{-1} biochar, CC: controlled irrigation +40 t ha^{-1} biochar, FA: flooding irrigation +0 t ha^{-1} biochar.

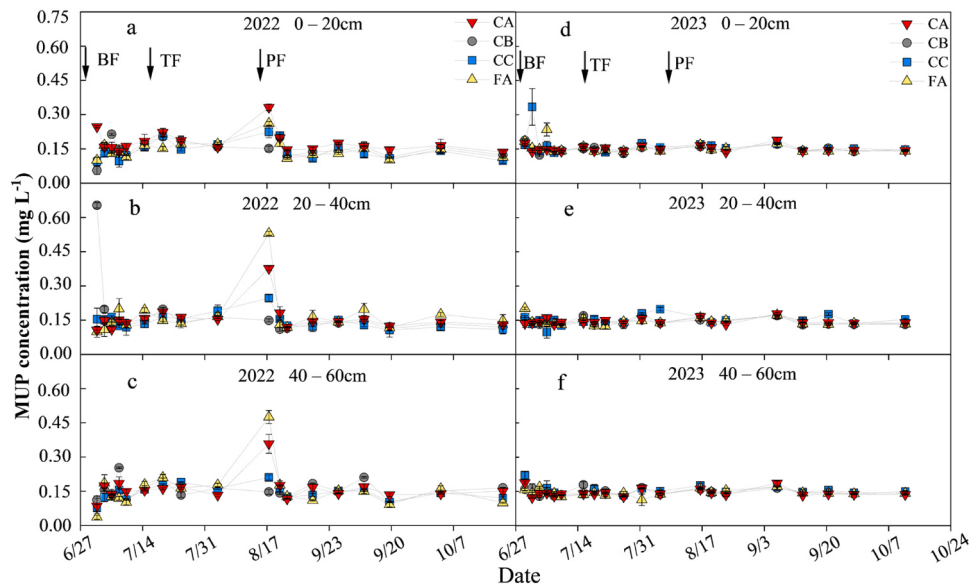


Fig. 6. Concentration of molybdate unreactive P (MUP) in soil solution at different depths in 2022 and 2023. a, d: 0–20 cm; b, e: 20–40 cm; c, f: 40–60 cm. The standard error ($n = 3$) is indicated by the error bars. CA: controlled irrigation +0 t ha^{-1} biochar, CB: controlled irrigation +20 t ha^{-1} biochar, CC: controlled irrigation +40 t ha^{-1} biochar, FA: flooding irrigation +0 t ha^{-1} biochar.

to the FA treatment. Conversely, at a depth of 20–60 cm, the P concentrations were lower in the CA treatment than in the FA treatment. In 2023, however, the concentrations of P components under the CA treatment were lower than those under the FA treatment at all depths, although these differences were not statistically significant. Specifically, the CA treatment led to decreases in TP by approximately 0.64–2.22 %, MRP by 1.13–2.29 %, and MUP by 0.22–2.10 %, when compared to the FA treatment.

It is worth mentioning that the combined influence of biochar and water-saving irrigation differed based on the rate at which biochar was applied. Regardless of the biochar application rate in 2022, the combined use of biochar and water-saving irrigation resulted in an increase in TP concentration at the 0–20 cm depth and a decrease at the 20–40 cm depth, as compared to paddy fields without biochar under

conventional flooded irrigation. This outcome was in line with the effects seen when only water-saving irrigation was employed. However, in 2023, the effects of 20 t ha^{-1} + water-saving irrigation and 40 t ha^{-1} + water-saving irrigation on P components in the soil solution at various depths in the paddy fields were markedly different. Compared to 0 t ha^{-1} + flooded irrigation, the 20 t ha^{-1} + water-saving irrigation treatment resulted in lower P concentrations at all depths in 2023, while the 40 t ha^{-1} + water-saving irrigation treatment led to an increase in P concentrations at all depths. In 2023, compared to the FA treatment, the average concentrations of TP, MRP, and MUP in the CB treatment during the entire growth period decreased by 0.04–1.13 %, 0.44–1.53 %, and 0.20–3.25 %, respectively, while the CC treatment resulted in increases of 1.87–2.04 %, 0.01–0.65 %, and 4.65–6.05 %, respectively.

Table 1

The average concentration of total P (TP), molybdate reactive P (MRP), and molybdate unreactive P (MUP) for different treatments at different depths in 2022 and 2023 (mg L⁻¹, mean ± SD).

Year	Depth	Treatment	TP	MRP	MUP
2022	0–20 cm	CA	0.4939 ± 0.0087 a	0.3145 ± 0.0032 b	0.1794 ± 0.0068 a
		CB	0.4741 ± 0.0050 b	0.3214 ± 0.0041 b	0.1527 ± 0.0026 b
		CC	0.4772 ± 0.0024 ab	0.3343 ± 0.0014 a	0.1429 ± 0.0019 b
		FA	0.4665 ± 0.0002 b	0.3203 ± 0.0031 b	0.1462 ± 0.0031 b
	20–40 cm	CA	0.4731 ± 0.0023 b	0.3156 ± 0.0035 b	0.1575 ± 0.0015 ab
		CB	0.4982 ± 0.0040 a	0.3276 ± 0.0012 a	0.1707 ± 0.0047 a
		CC	0.4810 ± 0.0041 b	0.3352 ± 0.0034 a	0.1458 ± 0.0072 b
		FA	0.5065 ± 0.0043 a	0.3370 ± 0.0060 a	0.1695 ± 0.0072 a
	40–60 cm	CA	0.4742 ± 0.0076 a	0.3129 ± 0.0009 a	0.1613 ± 0.0073 a
		CB	0.4751 ± 0.0051 a	0.3183 ± 0.0060 a	0.1567 ± 0.0015 ab
		CC	0.4625 ± 0.0078 a	0.3184 ± 0.0025 a	0.1441 ± 0.0056 b
		FA	0.4796 ± 0.0034 a	0.3214 ± 0.0012 a	0.1582 ± 0.0037 ab
2023	0–20 cm	CA	0.4361 ± 0.0042 b	0.2843 ± 0.0021 b	0.1518 ± 0.0025 b
		CB	0.4409 ± 0.0014 b	0.2909 ± 0.0015 ab	0.1500 ± 0.0026 b
		CC	0.4551 ± 0.0029 a	0.2928 ± 0.0026 a	0.1623 ± 0.0031 a
		FA	0.4460 ± 0.0044 ab	0.2909 ± 0.0034 ab	0.1551 ± 0.0014 ab
	20–40 cm	CA	0.4309 ± 0.0014 b	0.2860 ± 0.0003 a	0.1448 ± 0.0012 b
		CB	0.4321 ± 0.0013 b	0.2880 ± 0.0021 a	0.1440 ± 0.0017 b
		CC	0.4417 ± 0.0010 a	0.2903 ± 0.0040 a	0.1515 ± 0.0031 a
		FA	0.4336 ± 0.0015 b	0.2893 ± 0.0022 a	0.1443 ± 0.0011 b
	40–60 cm	CA	0.4295 ± 0.0019 b	0.2850 ± 0.0007 b	0.1445 ± 0.0019 a
		CB	0.4338 ± 0.0050 ab	0.2847 ± 0.0004 b	0.1491 ± 0.0047 a
		CC	0.4428 ± 0.0046 a	0.2892 ± 0.0019 a	0.1536 ± 0.0041 a
		FA	0.4340 ± 0.0036 ab	0.2891 ± 0.0009 a	0.1448 ± 0.0027 a

Note: CA: controlled irrigation +0 t ha⁻¹ biochar, CB: controlled irrigation +20 t ha⁻¹ biochar, CC: controlled irrigation +40 t ha⁻¹ biochar, FA: flooding irrigation +0 t ha⁻¹ biochar.

3.3. Phosphorus leaching loss

The different treatments did not significantly alter the proportions of various P fractions in the leaching losses (Fig. 7). Between 2022 and 2023, the leaching loss of MRP accounted for approximately 65.75–68.45 % of the TP leaching losses, while MUP constituted about 31.55–34.25 % of the TP leaching losses. As noted in the previous section, the concentrations of TP and MUP in the soil solution across all treatments exhibited no significant changes over time, and the P content in the leachate remained similarly stable.

The cumulative leaching loss curves for each P fraction across all treatments over the two years showed no significant inflection points, instead displaying a relatively steady increase over time (Fig. 7). The results from both years indicate that the irrigation method has a more pronounced effect on the leaching losses of P fractions than the application of biochar. There were no statistically significant differences in the leaching losses of various P forms under different biochar application rates in water-saving irrigated rice fields. In contrast, the leaching losses of P fractions in flooded irrigated rice fields were significantly higher than those in water-saving irrigated rice fields, regardless of biochar application (Fig. 7, Table 2). Compared to the FA treatment, the total cumulative leaching losses of TP for the CA, CB, and CC treatments were reduced by 41.32 % and 40.43 %, 41.81 % and 40.13 %, and 42.86 % and 39.08 % in 2022 and 2023, respectively. The cumulative leaching losses of MRP were significantly reduced by 41.29 % and 40.75 %, 40.47 % and 40.75 %, and 40.79 % and 40.25 %, respectively. Meanwhile, the cumulative leaching losses of MUP were significantly reduced by 41.38 % and 39.78 %, 44.42 % and 38.85 %, and 46.90 % and 36.69 %.

3.4. Phosphorus uptake by rice plants

Over a two-year period, P absorption by rice across different treatments demonstrated the trend of CC > CB > CA > FA (Fig. 8). Compared to flooding irrigation, controlled irrigation increased P absorption by 0.88–6.53 %. In paddy fields lacking biochar application, P uptake in the aboveground parts of rice increased by 7.31–7.55 % and 11.19–15.72 % at application rates of 20 t ha⁻¹ and 40 t ha⁻¹, respectively. When

compared to paddy fields under flooding irrigation alone, the combined application of water-saving irrigation and biochar led to increases in P uptake of 8.50–14.32 % for the CB treatment and 16.73–18.46 % for the CC treatment in the aboveground parts of the plants.

4. Discussion

4.1. The role of partially labile P pools in enhancing sustainable rice cultivation

According to their efficiency, soil P pools can be divided into three categories: labile P, partially labile P, and stable P, as suggested by studies conducted by Hu et al. (2016) and Redel et al. (2019). Various research efforts have pointed out that partially labile P constitutes the main component of P pools in paddy soils, whereas the contents of both labile and stable phosphorus are generally on the lower side, as noted by Ahmed et al. (2019). Our research findings support this conclusion. In this study, partially labile P represented approximately 51.82–73.03 % of the TP in the soil, significantly exceeding the contributions from labile and stable P. The presence and proportion of these P components significantly affect the availability of P in soil. An increased proportion of labile P boosts the potential for providing P in solution, which is essential for crop growth. However, the precise role of this substantial portion of partially labile P in paddy fields remains uncertain.

This study found that variations in total P content are closely related to the partially labile P component. For instance, in 2023, water-saving irrigation significantly increased total P at a 0–40 cm depth while decreasing it at a 40–60 cm depth, which correspondingly affected the content of partially labile P at these depths. In 2022, applying 40 t ha⁻¹ of biochar alongside with water-saving irrigation led to significant increases in total P content across the entire soil profile, alongside increases in both labile and partially labile P content. Furthermore, this study conducted redundancy analysis and correlation analysis of each P component constituting the soil P pool in relation to plant uptake and P leaching loss (Fig. 9). The results indicated that variations in plant P uptake were primarily influenced by dil.HCl-P and NaHCO₃-P_o. Specifically, P uptake by rice showed a significant negative correlation with both dil.HCl-P and NaHCO₃-P_o ($p < 0.05$). Among these, dil.HCl-P is the

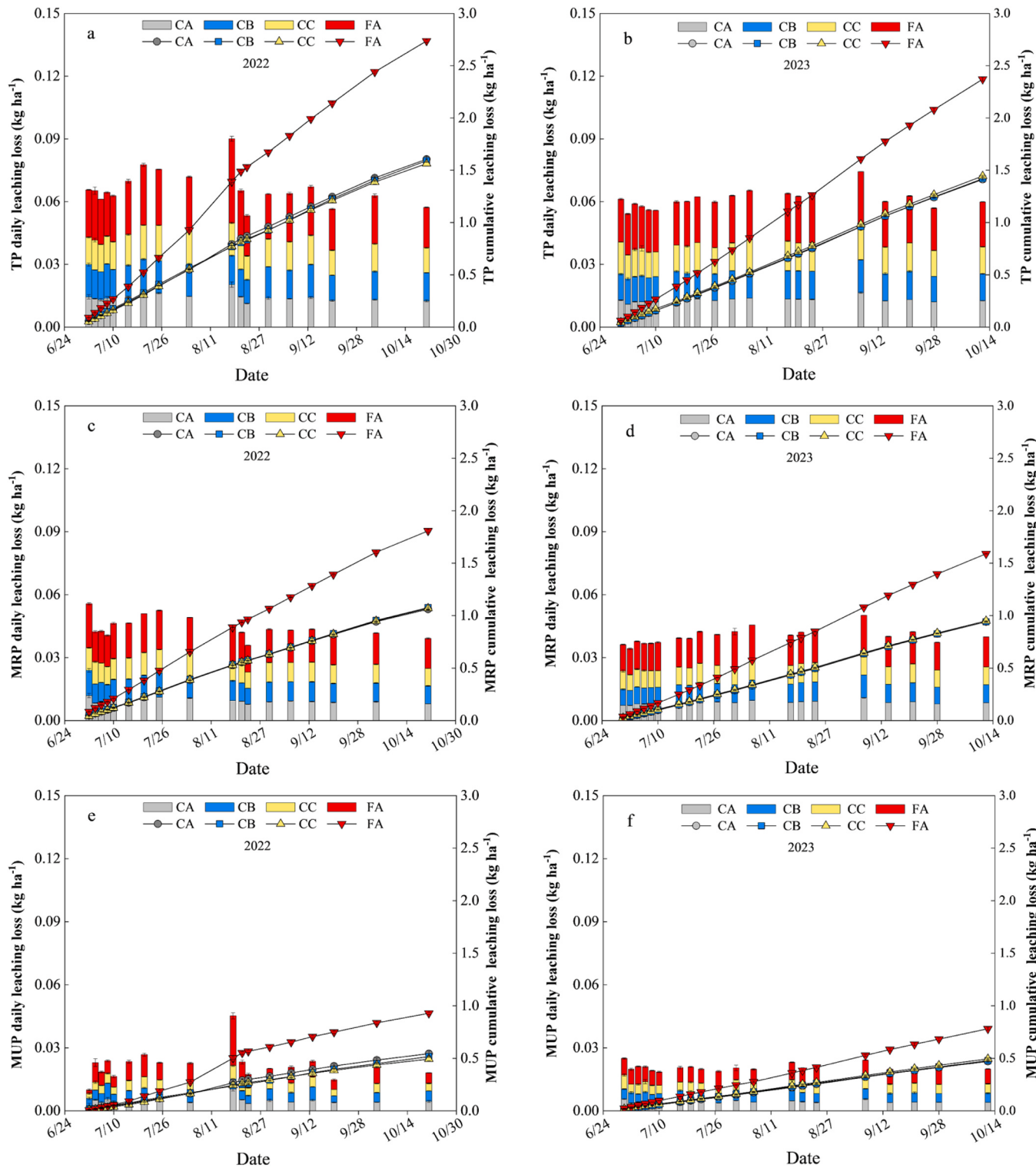


Fig. 7. The leaching loss of total P (TP), molybdate reactive P (MRP), and molybdate unreactive P (MUP) for different treatments in 2022 (a, c, e) and 2023 (b, d, f). The bar chart represents the daily P leaching loss, while the line chart represents the cumulative P leaching loss. CA: controlled irrigation +0 t ha⁻¹ biochar, CB: controlled irrigation +20 t ha⁻¹ biochar, CC: controlled irrigation +40 t ha⁻¹ biochar, FA: flooding irrigation +0 t ha⁻¹ biochar.

main component of partially labile P, accounting for approximately 67.86–89.57 % of this fraction. This suggests that partially labile P serves as a key source of effective P for rice in paddy fields. These findings are supported by Wang et al. (2016b) and Xu et al. (2020). For example, Wang et al. (2016b) demonstrated through pot experiments that continuous P application significantly affects the partially labile inorganic P component in paddy fields. Additionally, Yan et al. (2022)

indicated that reducing HCl-extractable P helped maintain stable effective P levels in a rapeseed-rice rotation system. This implies that effective consumption of soil HCl-extractable P pools is a major factor in sustaining stable levels of effective P in the soil. They suggested that HCl-extractable P, apart from H₂O-extractable P, is an important source of P for crop utilization. Although HCl-extractable P is calcium-bound and generally has low plant availability, plants can improve their

Table 2

The cumulative leaching loss of total P (TP), molybdate reactive P (MRP), and molybdate unreactive P (MUP) for different treatments in 2022 and 2023 (kg ha^{-1} , mean \pm SD).

Year	Treatment	TP	MRP	MUP
2022	CA	1.6061 ± 0.0277 b	1.0615 ± 0.0036 b	0.5447 ± 0.0242 b
	CB	1.5927 ± 0.0168 b	1.0763 ± 0.0217 b	0.5164 ± 0.0063 b
	CC	1.5639 ± 0.0227 b	1.0705 ± 0.0080 b	0.4933 ± 0.0152 b
	FA	2.7371 ± 0.0117 a	1.8080 ± 0.0112 a	0.9291 ± 0.0102 a
2023	CA	1.4126 ± 0.0069 b	0.9420 ± 0.0024 b	0.4707 ± 0.0067 b
	CB	1.4198 ± 0.0150 b	0.9419 ± 0.0011 b	0.4779 ± 0.0143 b
	CC	1.4447 ± 0.0080 b	0.9499 ± 0.0038 b	0.4948 ± 0.0103 b
	FA	2.3713 ± 0.0186 a	1.5898 ± 0.0038 a	0.7815 ± 0.0157 a

Note: CA: controlled irrigation $+0 \text{ t ha}^{-1}$ biochar, CB: controlled irrigation $+20 \text{ t ha}^{-1}$ biochar, CC: controlled irrigation $+40 \text{ t ha}^{-1}$ biochar, FA: flooding irrigation $+0 \text{ t ha}^{-1}$ biochar.

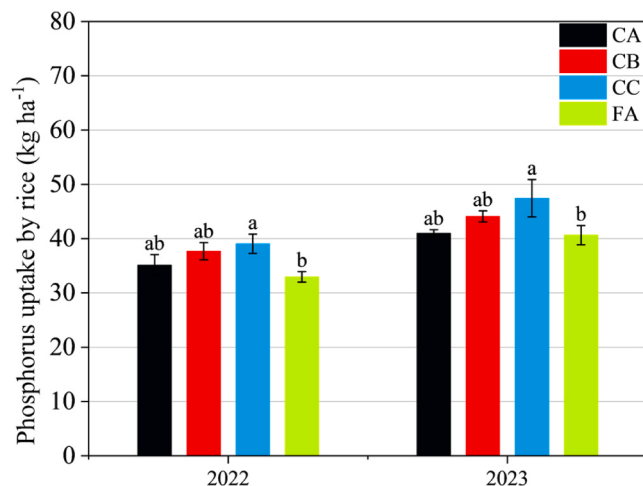


Fig. 8. P uptake by rice at harvest of all treatments. The difference among treatments is indicated by lowercase letters ($p < 0.05$). The error bars represent the standard error ($n = 3$). Note: CA: controlled irrigation $+0 \text{ t ha}^{-1}$ biochar, CB: controlled irrigation $+20 \text{ t ha}^{-1}$ biochar, CC: controlled irrigation $+40 \text{ t ha}^{-1}$ biochar, FA: flooding irrigation $+0 \text{ t ha}^{-1}$ biochar.

efficiency in absorbing nutrients by modifying their root morphology and physiological traits (Shen et al., 2011). Furthermore, microbial activity can activate less available inorganic P. Consequently, partially labile P becomes the primary source of P for crop uptake in soils with

low levels of available P (Daroub et al., 2001; Guo et al., 2008).

4.2. Water-saving irrigation impact on phosphorus dynamics

Water-saving irrigation (WSI) is in accordance with the 2030 Agenda's Sustainable Development Goals and is considered a promising approach for achieving sustainable rice production (Wang et al., 2016a; Akter et al., 2018; Zheng et al., 2018). Currently, WSI practices are being increasingly adopted worldwide. These techniques alter the soil's physical characteristics, influence microbial activity, and affect the growth of rice roots (Akter et al., 2018). Through the careful management of irrigation and drainage timing, duration, and volume, WSI has proven effective in preserving water resources, increasing crop yields, and mitigating pollution (Mao, 2002; Zhuang et al., 2019). Nevertheless, there remains inadequate evidence on the effects of wetting and drying cycles triggered by WSI on the spatial and temporal patterns of solid-phase P in the soil. Furthermore, it is crucial to determine whether these changes directly affect P leaching losses and P uptake by rice.

This study conducted a two-year investigation of rice cultivation in WSI fields, tracking the dynamics of P in the paddy soil. Although the effects of water-saving irrigation on P in the soil and soil solution were not entirely consistent over the two years, a consistent finding was that WSI irrigation significantly reduced the total P content at 40–60 cm depth. It also lowered various P components in the soil solution at 20–60 cm depths while significantly decreasing P leaching losses compared to flooded irrigation. Several scholars have offered explanations for this phenomenon (Jiang et al., 2021a). From the perspective of flooded irrigation, the larger volume and frequency of irrigation create a greater driving force for water infiltration, facilitating the migration of P

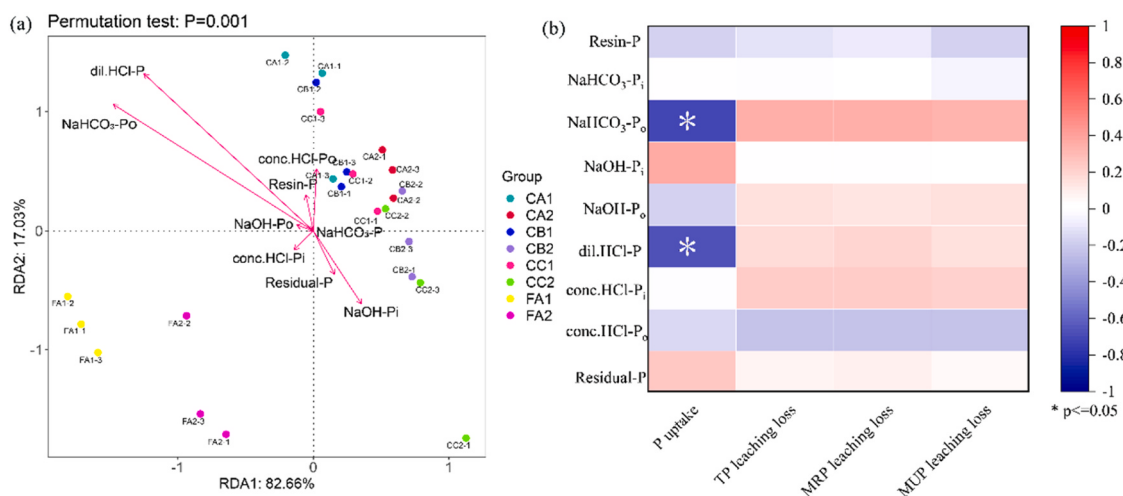


Fig. 9. Redundancy analysis (a) and correlation diagram (b) between P leaching, P uptake by rice and P fractionation. Note: CA: controlled irrigation $+0 \text{ t ha}^{-1}$ biochar, CB: controlled irrigation $+20 \text{ t ha}^{-1}$ biochar, CC: controlled irrigation $+40 \text{ t ha}^{-1}$ biochar, FA: flooding irrigation $+0 \text{ t ha}^{-1}$ biochar. The subscript numerals 1 and 2 denote observational results for the years 2022 and 2023, respectively.

to deeper soil layers. Additionally, the anaerobic conditions established by flooded irrigation can release P from the solid phase into the soil solution through the reduction of iron oxides. Consequently, fields that use flooded irrigation often have higher levels of P in the soil solution than those that adopt water-saving irrigation methods. Therefore, it is not surprising that flooded irrigation fields experience greater P leaching losses given the significant driving force for water infiltration and the elevated P levels in the soil solution.

It is widely accepted that the P content in the soil solution serves as the most direct source of P for plants. Surprisingly, the elevated concentrations of P in the soil solution resulting from flooded irrigation did not result in higher P uptake by rice when compared to water-saving irrigation. This finding contradicts the nutrient balance mechanisms proposed by researchers such as Lucci. (2019) and Gao et al. (2020), who argued that reduced soil moisture decreases ion diffusion rates and limits the accessibility of active nutrients to microbes, ultimately affecting the spatial availability of nutrients and reducing plant P absorption. Conversely, some studies suggest that aerobic microorganisms, such as arbuscular mycorrhizal fungi and P-solubilizing bacteria, exhibit enhanced activity due to improved aeration conditions resulting from drying and rewetting cycles (Butterly et al., 2009). This activity, in turn, can increase the availability and uptake of P by rice. However, in conditions with poor aeration, the intensity of P uptake by rice roots driven by microbial activity may be significantly diminished. This perspective helps clarify our confusion regarding the capability of plant roots to absorb P. Furthermore, Erinle et al. (2018) provided a more comprehensive explanation for the phenomena observed in our study by examining changes in soluble P levels. They indicated that the rewetting phase during drying and wetting cycles can lead to a temporary increase in P concentration in the soil solution. Although the window of opportunity for plant absorption is brief, the repetitive cycles of drying and rewetting induced by WSI are more likely to deplete the P pool than sustained wet conditions. Soil P content, microbial activity, root exudates, and root morphology all directly affect the P uptake capacity of rice (Raghothama and Karthikeyan, 2005; Noguera et al., 2010; Ali et al., 2020). More comprehensive research is needed to explore the mechanism of the non-reduction of P uptake in rice under WSI.

Low P use efficiency and the risk of P leaching due to accumulated P are widespread issues in most paddy fields. Water-saving irrigation is recognized for its significant water conservation capability, and its effectiveness in reducing leaching losses is well established. However, it is particularly noteworthy that, alongside reducing leaching losses, water-saving irrigation appears to enhance P uptake by rice plants. This study highlights the feasibility of widespread implementation of water-saving irrigation as a strategy for minimizing P loss in paddy fields and improving P use efficiency.

4.3. The effects of biochar on phosphorus dynamics in water-saving irrigated rice paddies are influenced by both the timing and dosage of its application

In recent years, pyrolysis-based carbonization technology has effectively bridged the beginning and end of the agricultural circular chain, serving as an efficient method for the resource utilization of waste biomass (Aller, 2016; Uddin et al., 2018). Through pyrolytic carbonization, agricultural waste is converted into biochar, which can directly supply P as an effective nutrient source to the soil, thereby participating in various stages of the soil P cycle (Xu et al., 2014). Numerous studies have demonstrated that biochar releases significant amounts of available P, promoting plant growth and enhancing crop yields (Chen et al., 2022). The findings in this instance reveal that, in 2022, paddy fields that received a biochar application rate of 40 t ha^{-1} had a significantly elevated P content within the 0–60 cm soil depth compared to fields that did not receive any biochar treatment. Applying 20 t ha^{-1} of biochar led to an increase in total P content only in the top 40 cm of soil during the initial and mid-stages of rice growth, but it resulted in a decrease in total

P content in the soil between 40 and 60 cm deep. However, at harvest time, the total P content between 40 and 60 cm depth was found to be increased. While the total P content rose with biochar treatment, P absorption by rice increases (increased by 7.31–11.19%). Therefore, it can be concluded that during the first year following biochar application, its ability to release rich available P played a crucial role throughout the rice growth period. However, this release effect was not observed in the second year after application. The ability of biochar to rapidly release P was demonstrated by Qian et al. (2013), who found that nearly 50 % of the P in biochar was released within the first 8 h, primarily as pyrophosphate and orthophosphate. However, once the labile P pool in biochar has been depleted, the remaining P is largely stable. This observation aligns with the findings of Liang et al. (2014), who described the P release process in soil as occurring in two stages: an initial direct diffusion of labile P into the soil, followed by a slow and continuous dissolution of the more stable P. In other words, biochar exhibits a “rapid release–slow replenishment” pattern in its P supply capacity. These insights indicate that biochar can serve as an effective short-term P supplement for P-deficient soils.

In 2023, the P content in paddy fields with biochar application showed varying degrees of reduction compared to untreated fields at different soil profile depths, particularly during the middle to late stages of rice growth. Notably, the stable P and partially labile P components also decreased alongside the total P content. The P uptake by rice in the biochar-treated fields in 2023 remained higher than that in untreated fields, indicating that biochar effectively demonstrated its capacity to activate soil P in the second year after application. More studies are necessary to understand the processes by which it triggers the activation of stable and partially labile P, whether via dissolution or through mineralization. This strong activation ability can be a double-edged sword, as excessive activation may increase the risk of leaching. Although the results from both years of experimentation indicate that both 20 t ha^{-1} and 40 t ha^{-1} biochar combined with water-saving irrigation can promote P uptake by rice plants and reduce P leaching losses compared to flooded irrigation, the 40 t ha^{-1} biochar with water-saving irrigation only reduces leaching losses by decreasing the volume of leachate compared to flooded irrigation. This management practice leads to a surplus of P in the soil solution. When compared to flooded irrigation, applying water-saving irrigation in conjunction with a 40 t ha^{-1} biochar application led to increases in soil solution TP content by 2.04 % at 0–20 cm depth, 1.87 % at 20–40 cm depth ($p < 0.05$), and 2.02 % at 40–60 cm depth in 2023. Meanwhile, the combination of 20 t ha^{-1} biochar with water-saving irrigation reduced the P content in the soil solution while also decreasing leachate volume, allowing for better utilization of the activated P. Considering P availability and the reduction of environmental P pollution risk, the combination of 20 t ha^{-1} biochar with water-saving irrigation is a more suitable field management practice. Several previous studies have investigated biochar and WSI in other agroecological contexts. For instance, Chen et al. (2021) demonstrated that a biochar application rate of 40 t ha^{-1} under WSI conditions significantly improved irrigation water use efficiency in paddy rice systems. Similarly, Zhang et al. (2024) reported that the combination of WSI with reduced nitrogen fertilization (10 % reduction) and 12.5 t ha^{-1} biochar application enhanced both water-nitrogen use efficiency and grain yield in cold-region black soil paddy fields. These variations in optimal application rates are likely attributable to differences in multiple factors including biochar characteristics, soil properties, and irrigation management practices. Our study provides novel insights by specifically examining P loss and P uptake mediated by soil P pools in paddy fields applying biochar and WSI together, which has not been thoroughly investigated in previous work. Future studies could further explore the effectiveness of biochar in regulating P dynamics in rice paddies under water-saving irrigation by implementing multiple biochar application rates.

Additionally, the long-term implications of repeated biochar application on soil health and P dynamics remain uncertain (Aller et al.,

2017). For instance, while biochar may initially enhance P retention, its aging effects could alter P availability over time (Qin et al., 2022). Furthermore, depending on feedstock and pyrolysis conditions, biochar may introduce heavy metals (e.g., Cd, Pb) (Huang et al., 2021) or alter soil microbial communities (Palansooriya et al., 2019), potentially affecting nutrient cycling. Future studies should monitor multi-year biochar impacts under field conditions, including soil quality indicators (e.g., organic matter, microbial biomass) (Jiang et al., 2019) and environmental risk assessments (e.g., heavy metal accumulation (Su et al., 2021)).

5. Conclusion

Based on two years of field experiments, this study investigated the distribution characteristics of various P forms in both solid and liquid phases of paddy soils under biochar application and water-saving irrigation, focusing on their vertical profiles and seasonal variations, as well as rice P uptake and P leaching losses. The effects of biochar exhibited significant interannual variation: in 2022, the application of biochar at 20, 40 t ha⁻¹ significantly increased TP content across soil layers (by 4.91–17.40 %), and 40 t ha⁻¹ biochar enhanced labile P (6.52–66.47 %) and partially labile P (5.68–24.08 %). In contrast, in 2023, TP content generally decreased (by 1.07–21.79 %), mainly due to reductions in partially labile P and stable P fractions. Soil solution analysis revealed that MRP, accounting for 37.88–95.76 % of TP, exhibited distinct seasonal fluctuations, while TP and MUP remained relatively stable. Notably, biochar at 40 t ha⁻¹ in 2023 significantly increased P concentrations in soil solution layers (TP increased by 2.52–4.36 %). Biochar in water-saving irrigated paddy fields manifests a "rapid release–slow replenishment" pattern of phosphorus release. The combination of 20 t ha⁻¹ biochar with water-saving irrigation effectively decreased P redundancy in the soil solution, facilitating improved P uptake by rice, making it a recommended field management practice. While research has confirmed the positive regulation of biochar on P in water-saving irrigated rice fields, the large-scale application of biochar in farmland must also consider other environmental impacts it may bring, such as the introduction of heavy metals. Long-term tracking of biochar's environmental effects in water-saving irrigated rice fields remains essential to evaluate its role in addressing global P sustainability challenges, such as optimizing use efficiency and reducing ecological losses.

CRediT authorship contribution statement

Shufang Wang: Formal analysis. **Shihong Yang:** Writing – review & editing, Supervision, Funding acquisition. **Pengfei Zhang:** Methodology. **Qian Huang:** Methodology. **JingCheng Zhu:** Methodology. **Jin Li:** Methodology. **Zewei Jiang:** Writing – review & editing, Data curation. **Yi Xu:** Writing – review & editing, Validation. **Jie Zhang:** Writing – review & editing. **Lili Zhu:** Methodology. **Suting Qi:** Writing – original draft, Software, Data curation, Conceptualization.

Declaration of Competing Interest

The authors declare that they have no known competing financial interests or personal relationships that could have appeared to influence the work reported in this paper.

Acknowledgments

This work was supported by the National Natural Science Foundation of China (52379038), the Postgraduate Research & Practice innovation Program of Jiangsu Province (KYCX23_0738), the Key Research and Development Plan of Jiangsu Province (BE2022390).

Appendix A. Supporting information

Supplementary data associated with this article can be found in the online version at doi:10.1016/j.agee.2025.109864.

Data availability

Data will be made available on request.

References

- Abdala, D.B., da Silva, I.R., Vergütz, L., Sparks, D.L., 2015. Long-term manure application effects on phosphorus speciation, kinetics and distribution in highly weathered agricultural soils. *Chemosphere* 119, 504–514.
- Ahmed, W., Huang, J., Kaillou, L., Qaswar, M., Khan, M.N., Chen, J., Sun, G., Huang, Q.H., Liu, Y.R., Liu, G.R., Sun, M., Li, C., Li, D.C., Ali, S., Normatov, Y., Mehmood, S., Zhang, H.M., 2019. Changes in phosphorus fractions associated with soil chemical properties under long-term organic and inorganic fertilization in paddy soils of southern China. *Plos One* 14, e0216881.
- Akter, M., Deroo, H., Kamal, A.M., Kader, M.A., Verhoeven, E., Decock, C., Boeckx, P., Sleutel, S., 2018. Impact of irrigation management on paddy soil N supply and depth distribution of abiotic drivers. *Agric. Ecosyst. Environ.* 261, 12–24.
- Ali, I., He, L., Ullah, S., Quan, Z., Wei, S.Q., Igbal, A., Munsif, F., Shah, T., Xuan, Y., Luo, Y.O., Li, T.Y., Jiang, L.G., 2020. Biochar addition coupled with nitrogen fertilization impacts on soil quality, crop productivity, and nitrogen uptake under double-cropping system. *Food Energy Secur.* 9, e208.
- Aller, D., Mazur, R., Moore, K., Hintz, R., Laird, D., Horton, R., 2017. Biochar age and crop rotation impacts on soil quality. *Soil Sci. Soc. Am. J.* 81, 1157–1167.
- Aller, M.F., 2016. Biochar properties: transport, fate, and impact. *Crit. Rev. Environ. Sci. Technol.* 46, 1183–1296.
- Butterly, C.R., Büinemann, E.K., McNeill, A.M., Baldock, J.A., Marschner, P.J.S.B., 2009. Carbon pulses but not phosphorus pulses are related to decreases in microbial biomass during repeated drying and rewetting of soils. *Biochemistry* 41, 1406–1416.
- Chen, H., Yuan, J.H., Chen, G.L., Zhao, X., Wang, S.Q., Wang, D.J., Wang, L., Wang, Y.J., Wang, Y., 2022. Long-term biochar addition significantly decreases rice rhizosphere available phosphorus and its release risk to the environment. *Biochar* 4, 54.
- Chen, X., Yang, S.H., Ding, J., Jiang, Z.W., Sun, X., 2021. Effects of biochar addition on rice growth and yield under water-saving irrigation. *Water* 13, 209.
- Condron, L.M., Newman, S., 2011. Revisiting the fundamentals of phosphorus fractionation of sediments and soils. *J. Soils Sediment.* 11, 830–840.
- Daroub, S.H., Ellis, B.G., Robertson, G.P., 2001. Effect of cropping and low-chemical input systems on soil phosphorus fractions. *Soil Sci.* 166, 281–291.
- Erinle, K.O., Li, J.Q., Doolette, A., Marschner, P., 2018. Soil phosphorus pools in the detritusphere of plant residues with different C/P ratio-influence of drying and rewetting. *Biol. Fertil. Soils* 54, 841–852.
- Gao, D.C., Bai, E., Li, M.H., Zhao, C.H., Yu, K.L., Hagedorn, F., 2020. Responses of soil nitrogen and phosphorus cycling to drying and rewetting cycles: a meta-analysis. *Soil Biol. Biochem.* 148, 107896.
- Guo, S.L., Dang, T.H., Hao, M.D., 2008. Phosphorus changes and sorption characteristics in a calcareous soil under long-term fertilization. *Pedosphere* 18, 248–256.
- Hedley, M.J., Stewart, J.W.B., Chauhan, B.S., 1982b. Changes in inorganic and organic soil phosphorus fractions induced by cultivation practices and by laboratory incubations. *Soil Sci. Soc. Am. J.* 46, 970–976.
- Hedley, M.J., Stewart, J.W.B., Chauhan, B.S., 1982a. Changes in inorganic and organic soil phosphorus fractions induced by cultivation practices and by laboratory incubations1. *Soil Sci. Soc. Am. J.* 46, 970–976.
- Hou, E.Q., Chen, C.R., Kuang, Y.W., Zhang, Y.G., Heenan, M., Wen, D.Z., 2016. A structural equation model analysis of phosphorus transformations in global unfertilized and uncultivated soils. *Glob. Biogeochem. Cycles* 30, 1300–1309.
- Hu, B., Yang, B., Pang, X.Y., Bao, W.K., Tian, G.L., 2016. Responses of soil phosphorus fractions to gap size in a reforested spruce forest. *Geoderma* 279, 61–69.
- Huang, R., Ji, X., Wang, X., Chen, H., Wei, W., Liu, S., Xie, Y., 2021. Synchronous passivation and absorption inhibition of Cd-As co-contamination in soil-rice system: a review. *J. AgroEnviron. Sci.* 40, 482–492.
- Jia, W., Yu, Z., Chen, J., Zhang, J., Zhu, J., Yang, W., Yang, R., Wu, P., Wang, S., 2024. Synergistic effect between biochar and nitrate fertilizer facilitated arsenic immobilization in an anaerobic contaminated paddy soil. *Sci. Total Environ.* 955, 177007.
- Jiang, B.S., Shen, J.L., Sun, M.H., Hu, Y.J., Jiang, W.Q., Wang, J., Li, Y., Wu, J.S., 2021a. Soil phosphorus availability and rice phosphorus uptake in paddy fields under various agronomic practices. *Pedosphere* 31, 103–115.
- Jiang, X.Y., Tan, X.P., Cheng, J., Haddix, M.L., Cotrufo, M.F., 2019. Interactions between aged biochar, fresh low molecular weight carbon and soil organic carbon after 3.5 years soil-biochar incubations. *Geoderma* 333, 99–107.
- Jiang, Z.W., Yang, S.H., Pang, Q.Q., Xu, Y., Chen, X., Sun, X., Qi, S.T., Yu, W.Q., 2021b. Biochar improved soil health and mitigated greenhouse gas emission from controlled irrigation paddy field: insights into microbial diversity. *J. Clean. Prod.* 318, 128595.
- Kruse, J., Abraham, M., Amelung, W., Baum, C., Bol, R., Kühn, O., Lewandowski, H., Niederberger, J., Oelmann, Y., Rüger, C., Santner, J., Siebers, M., Siebers, N., Spohn, M., Vestergren, J., Vogts, A., Leinweber, P., 2015. Innovative methods in soil phosphorus research: a review. *J. Plant Nutr. Soil Sci.* 178, 43–88.

- Liang, Y., Cao, X.D., Zhao, L., Xu, X.Y., Harris, W., 2014. Phosphorus release from dairy manure, the manure-derived biochar, and their amended soil: effects of phosphorus nature and soil property. *J. Environ. Qual.* 43, 1504–1509.
- Liu, J., Yang, J.J., Cade-Menun, B.J., Liang, X.Q., Hu, Y.F., Liu, C.W., Zhao, Y., Li, L., Shi, J.Y., 2013. Complementary phosphorus speciation in agricultural soils by sequential fractionation, solution ^{31}P nuclear magnetic resonance, and phosphorus K-edge X-ray absorption near-edge structure spectroscopy. *J. Environ. Qual.* 42, 1763–1770.
- Lucci, G.M., 2019. Pastures and drought: a review of processes and implications for nitrogen and phosphorus cycling in grassland systems. *Soil Res.* 57, 101–112.
- Mao, Z., 2002. Water saving irrigation for rice and its effect on environment. *Eng. Sci.* 4, 8–16.
- Matin, N.H., Jalali, M., Antoniadis, V., Shaheen, S.M., Wang, J.X., Zhang, T., Wang, H.L., Rinklebe, J., 2020. Almond and walnut shell-derived biochars affect sorption-desorption, fractionation, and release of phosphorus in two different soils. *Chemosphere* 241, 124888.
- Miao, H., Qiao, Y., Tang, Y., Feng, Q., Yue, Y., Xue, H., Miao, S., 2023. Effects of straw and biochar return on the apparent utilization efficiency of phosphorus in rice under the condition of short-time rainstorm. *Res. Soil Water Conserv.* 30, 241–246.
- Motavalli, P.P., Miles, R.J., 2002. Soil phosphorus fractions after 111 years of animal manure and fertilizer applications. *Biol. Fertil. Soils* 36, 35–42.
- Murphy, J., Riley, J.P., 1962. A modified single solution method for the determination of phosphate in natural waters. *Anal. Chim. Acta* 27, 678–681.
- Negassa, W., Leinweber, P., 2009. How does the Hedley sequential phosphorus fractionation reflect impacts of land use and management on soil phosphorus: a review. *J. Plant Nutr. Soil Sci.* 172, 305–325.
- Noguera, D., Rondón, M., Laossi, K.R., Hoyos, V., Lavelle, P., de Carvalho, M.H.C., Barot, S., 2010. Contrasted effect of biochar and earthworms on rice growth and resource allocation in different soils. *Soil Biol. Biochem.* 42, 1017–1027.
- Palansooriya, K.N., Wong, J.T.F., Hashimoto, Y., Huang, L.B., Rinklebe, J., Chang, S.X., Bolan, N., Wang, H.L., Ok, Y.S., 2019. Response of microbial communities to biochar-amended soils: a critical review. *Biochar* 1, 3–22.
- Qi, S.T., Yang, S.H., Xu, Y., Hu, J.Z., Qiu, H.N., Jiang, Z.W., Zhang, M.R., Yu, W.Q., 2024. Enhanced available phosphorus in paddy fields applying biochar and water-saving irrigation together: the role of alkaline phosphomonoesterase-harboring microorganisms. *J. Environ. Manag.* 371, 123260.
- Qian, T.T., Zhang, X.S., Hu, J.Y., Jiang, H., 2013. Effects of environmental conditions on the release of phosphorus from biochar. *Chemosphere* 93, 2069–2075.
- Qin, G.B., Yan, X., Wei, J.J., Wu, J.F., Wei, Z.Q., 2022. Does the carbon skeleton of biochar contribute to soil phosphate sorption? A case study from paddy soils with woody biochar amendment. *Soil Res.* 60, 242–251.
- Raghothama, K.G., Karthikeyan, A.S., 2005. Phosphate acquisition. *Plant Soil* 274, 37–49.
- Redel, Y., Staunton, S., Durán, P., Gianfreda, L., Rumpel, C., Mora, M.D., 2019. Fertilizer P uptake determined by soil P fractionation and phosphatase activity. *J. Soil Sci. Plant Nutr.* 19, 166–174.
- Shen, J.B., Yuan, L.X., Zhang, J.L., Li, H.G., Bai, Z.H., Chen, X.P., Zhang, W.F., Zhang, F.S., 2011. Phosphorus dynamics: from soil to plant. *Plant Physiol.* 156, 997–1005.
- Su, Y.F., Wen, Y.J., Yang, W.J., Zhang, X., Xia, M., Zhou, N., Xiong, Y.F., Zhou, Z., 2021. The mechanism transformation of ramie biochar's cadmium adsorption by aging. *Bioresour. Technol.* 330, 124947.
- Sun, B., Li, S., Zhou, Y., Zhang, Y., Chen, J., Liu, T., Guo, J., Ling, N., Guo, S., 2020. Effects of optimized fertilization on rice yield and accumulation and distribution of phosphorus under different rotation systems. *J. Nanjing Agric. Univ.* 43, 658–666.
- Tiessen, H., Moir, J.O., 1993. Characterization of Available P by Sequential Extraction. CRC Press.
- Uddin, M.N., Techato, K., Taweekun, J., Rahman, M.M., Rasul, M.G., Mahlia, T.M.I., Ashraful, S.M., 2018. An overview of recent developments in biomass pyrolysis technologies. *Energies* 11, 3115.
- Wang, J.X., Wang, B.Y., Bian, R.J., He, W.J., Liu, Y., Shen, G.C., Xie, H.F., Feng, Y.F., 2024. Bibliometric analysis of biochar-based organic fertilizers in the past 15 years: focus on ammonia volatilization and greenhouse gas emissions during composting. *Environ. Res.* 243, 117853.
- Wang, X.H., Lu, W.X., Xu, Y.J., Zhang, G.X., Qu, W., Cheng, W.G., 2016a. The positive impacts of irrigation schedules on rice yield and water consumption: synergies in Jilin Province, Northeast China. *Int. J. Agric. Sustain.* 14, 1–12.
- Wang, Y., Zhao, X., Wang, L., Jin, S.Z., Zhu, W.B., Lu, Y.N., Wang, S.Q., 2016b. A five-year P fertilization pot trial for wheat only in a rice-wheat rotation of Chinese paddy soil: interaction of P availability and microorganism. *Plant Soil* 399, 305–318.
- Wu, Y.H., Liu, J.Z., Rene, E.R., 2018. Periphytic biofilms: a promising nutrient utilization regulator in wetlands. *Bioresour. Technol.* 248, 44–48.
- Xu, G., Sun, J.N., Shao, H.B., Chang, S.X., 2014. Biochar had effects on phosphorus sorption and desorption in three soils with differing acidity. *Ecol. Eng.* 62, 54–60.
- Xu, X.L., Mao, X.L., Van Zwieten, L., Niazi, N.K., Lu, K.P., Bolan, N.S., Wang, H.L., 2020. Wetting-drying cycles during a rice-wheat crop rotation rapidly (im)mobilize recalcitrant soil phosphorus. *J. Soils Sediment.* 20, 3921–3930.
- Yan, J.Y., Ren, T., Wang, K.K., Li, H.Z., Li, X.K., Cong, R.H., Lu, J.W., 2022. Improved crop yield and phosphorus uptake through the optimization of phosphorus fertilizer rates in an oilseed rape-rice cropping system. *Field Crops Res.* 286, 108614.
- Yang, X., Post, W.M., 2011. Phosphorus transformations as a function of pedogenesis: a synthesis of soil phosphorus data using Hedley fractionation method. *Biogeosciences* 8, 2907–2916.
- Zhang, Z., Zhou, L., Li, H., Kong, F., Lu, X., 2024. Effect of water-saving irrigation and nitrogen reduction combined with biochar application on photosynthetic characteristics and water and nitrogen utilization of rice. *Trans. Chin. Soc. Agric. Mach.* 55, 386.
- Zheng, J.L., Chen, T.T., Xia, G.M., Chen, W., Liu, G.Y., Chi, D.C., 2018. Effects of zeolite application on grain yield, water use and nitrogen uptake of rice under alternate wetting and drying irrigation. *Int. J. Agric. Biol. Eng.* 11, 157–164.
- Zhuang, Y.H., Zhang, L., Li, S.S., Liu, H.B., Zhai, L.M., Zhou, F., Ye, Y.S., Ruan, S.H., Wen, W.J., 2019. Effects and potential of water-saving irrigation for rice production in China. *Agric. Water Manag.* 217, 374–382.